



**HAL**  
open science

# Uncertainty Analysis for Day Ahead Power Reserve - Quantification in an Urban Microgrid Including PV Generators

Xingyu Yan, Dhaker Abbes, Bruno François

► **To cite this version:**

Xingyu Yan, Dhaker Abbes, Bruno François. Uncertainty Analysis for Day Ahead Power Reserve - Quantification in an Urban Microgrid Including PV Generators. *Renewable Energy*, 2017, 10.1016/j.renene.2017.01.022 . hal-01756824

**HAL Id: hal-01756824**

**<https://hal.science/hal-01756824v1>**

Submitted on 3 Apr 2018

**HAL** is a multi-disciplinary open access archive for the deposit and dissemination of scientific research documents, whether they are published or not. The documents may come from teaching and research institutions in France or abroad, or from public or private research centers.

L'archive ouverte pluridisciplinaire **HAL**, est destinée au dépôt et à la diffusion de documents scientifiques de niveau recherche, publiés ou non, émanant des établissements d'enseignement et de recherche français ou étrangers, des laboratoires publics ou privés.

# Uncertainty Analysis for Day Ahead Power Reserve Quantification in an Urban Microgrid Including PV Generators

Xingyu YAN<sup>1</sup>, Dhaker ABBES<sup>2</sup>, Bruno FRANCOIS<sup>1</sup>

Univ. Lille, Centrale Lille, Arts et Métiers Paristech, HEI, EA 2697 – L2EP – Laboratoire d’Electrotechnique et d’Electronique de Puissance,

F-59000 Lille, France

E-mail: [bruno.francois@ec-lille.fr](mailto:bruno.francois@ec-lille.fr)

**Abstract**—Setting an adequate operating power reserve (PR) to compensate unpredictable imbalances between generation and consumption is essential for power system security. Operating power reserve should be carefully sized but also ideally minimized and dispatched to reduce operation costs with a satisfying security level. Although several energy generation and load forecasting tools have been developed, decision-making methods are required to estimate the operating power reserve amount within its dispatch over generators during small time windows and with adaptive capabilities to markets, as new ancillary service markets. This paper proposes an uncertainty analysis method for power reserve quantification in an urban microgrid with a high penetration ratio of PV (photovoltaic) power. First, forecasting errors of PV production and load demand are estimated one day ahead by using artificial neural networks. Then two methods are proposed to calculate one day ahead the net demand error. The first perform a direct forecast of the error, the second one calculates it from the available PV power and load demand forecast errors. This remaining net error is analyzed with dedicated statistical and stochastic procedures. Hence, according to an accepted risk level, a method is proposed to calculate the required PR for each hour.

**Index Terms**— Power reserve scheduling; renewable energy sources; forecast errors; uncertainty analysis; reliability.

## I. INTRODUCTION

INCREASE of the electricity produced by renewable energy sources (RES) contributes to energy supply portfolio diversity and reduces the expanded use of fossil fuels. However, the energy production from RES is characterized by power intermittencies and production uncertainties, especially for PV and wind power. New operational challenges appear for grid operators like ramping and regulation requirements in addition to impacts on power system stability. Hence, grid codes evolve and in many European countries, renewable sources are more and more required to provide ancillary services for grid operators [1]. In order to maintain the security and reliability of grids with a high share of renewable generators, primary, secondary and tertiary regulation as well as spinning reserve are now required from renewable generators in more and more grid codes [2, 3]. This operating power reserve should be ideally minimized to reduce system costs with a satisfying security level.

Typically, PV power generation forecasting is needed to optimize the operation and to reduce the cost of power systems, especially for the scheduling and dispatching of required hourly operating [4]. However, the predicted uncertainty associated with forecast cannot be eliminated even with the best model tools. In addition to the load demand uncertainty, the combination of power generation and consumption variability with forecast uncertainty makes the situation more difficult for power system operators to schedule and to set power reserve level. Therefore, the uncertainties from both generation and consumption must be taken into account by an accurate stochastic model for power system management. In addition, forecasting errors from system uncertainty analysis could be used to set power reserve [5].

Historically, most conventional utilities have adopted deterministic criteria for the reserve requirement: the operating rules required PR to be greater than the capacity of the largest on-line generator or a fraction of the load, or equal to some function of both of them. Those deterministic criteria are widely used because of their simplicity and understandable employing. However,

39 these deterministic calculation methods are gradually replaced by probabilistic methods that respond to the stochastic factors  
40 corresponding to the system reliability. Several research works have been focused on calculating the total system uncertainty  
41 from all the variable sources. Based on dynamic simulations, the study in [8] is focusing on dynamic frequency control of an  
42 isolated system and the reduction of the impact due to large shares of wind and PV powers. However this work did not consider  
43 other aspects, such as variability and forecast accuracy. A deterministic approach is proposed in [9] to analyze the flexibility of  
44 thermal generation to balance wind power variations and prediction errors. A stochastic analysis could improve it in order to be  
45 able to quantify the power reserve with a risk index. A stochastic model was developed in [10] to simulate the operations and the  
46 line disconnection events of the transmission network due to overloads beyond the rated capacity. But the issue is clearly that  
47 analysis of the system states, in terms of power request and supply, are critical for network vulnerability and may induce a cascade  
48 of line disconnections leading to a massive network blackout. An insurance strategy is proposed in [11] to cover the possible  
49 imbalance cost that wind power producer may incur in electricity markets. Monte Carlo simulations have been used to estimate  
50 insurance premiums for further analysis excesses and so require a significant calculation time.

51 Our previous works in [6, 7] showed that forecasting errors from system uncertainty analysis could be used for PR setting.  
52 Following these promising results and experiences, we have carried out further investigations on rigorous methods to quantify  
53 the required PR. The task is to calculate it by considering uncertainties from PV prediction and load forecast or with uncertainty  
54 estimation. In the second part of this paper, PV power and load uncertainty and variability are analyzed. Then, the artificial  
55 neural network based prediction methods are applied to forecast PV power, load demand and errors. In the third part, the Net  
56 Demand (ND) Forecasted uncertainty is obtained, for each hour of the next day, as the difference between the forecasted  
57 production uncertainty and the forecasted load uncertainty. Two methods are detailed to calculate the ND forecast errors. An  
58 hourly probability density function of all predicted ND forecasted errors has been used for the error analysis. In the fourth part, a  
59 method is explained to assess the accuracy of these predictions and to quantify the required operating PR to compensate the  
60 system power unbalancing due to these errors. Power reserve is obtained by choosing a risk level related to two reliability  
61 assessment indicators: loss of load probability (LOLP), and expected energy not served (EENS). Finally, this management tool is  
62 proved through an illustrative example.

## 63 II.METHODOLOGY

### 64 *A.PV Power and Load Uncertainty Analysis*

65 The PV power variability is the expected change in generation while PV power uncertainty is the unexpected change from  
66 what was anticipated, such as a suddenly cloud cover. The former depends on the latitude and the rotation of Earth, while the  
67 latter is mostly caused by uncertainty conditions, such as cloud variations over the PV. The movement of clouds introduces a  
68 significant uncertainty that can result in rapid fluctuations in solar irradiance and therefore PV power output. However, the  
69 influence of a moving cloud and, hence, the shading of an entire PV site depends on the PV area, cloud speed, cloud height and  
70 many other factors. Data from solar installations covering a large spatial extent have an hourly temporal dynamic, while  
71 individual zones have instantaneous dynamics as in local distribution networks or micro grids.

72 The daily operation of a power system should be matched to load variations to maintain system reliability. This reliability  
73 refers to two areas:

- 74 - system adequacy, which depends on sufficient facilities within the system to satisfy system operational constraints and  
75 load demand, and
- 76 - system security, which is the system ability to respond to dynamic disturbances.

77 When RES represent a significant part of the power generation, system operating power reserve must be larger to regulate the  
 78 variations and maintain the security level. This additional power is required to stable the electrical network. Classically this  
 79 power reserve is provided by controllable generators (gas turbines, diesel plant, ..). Today, the increasing of balancing power  
 80 reserves leads to a significant increase in the power system operating cost and so system may limit the PV power penetration is  
 81 due to the variability and uncertainty over short time scales.

82 There are different ways to manage variability and uncertainty. In general, system operators and planners use mechanisms  
 83 including forecasting, scheduling, economic dispatch, and power reserves to ensure performances that satisfy reliability  
 84 standards with the least cost. The earlier system operators and planners know what kind of variability and uncertainty they will  
 85 have to deal with, the more options they will have to accommodate it and cheaper it will be. The key task of variability and  
 86 uncertainty management is to maintain a reliable operation of the power system (grid connected or isolated) while keeping down  
 87 costs.

88 Energy management of electrical systems is usually implemented over different time scales. One day ahead, system operators  
 89 have to balance the load demand with electrical generation by planning the starting and set points of controllable generators on  
 90 an hourly time step. Risks are also considered and thus a power reserve has also to be hourly planned. During the day,  
 91 unexpected PV power lack is compensated by injecting a primary power reserve. The PV variability can be separated into  
 92 different time scales associated with different impacts, onto the grid management and costs. Consequently, more capacity to  
 93 compensate errors in forecasts or unexpected events must be accommodated.

94 The instantaneous PV power output is affected by many correlated external and physical inputs, such as irradiance, humidity,  
 95 pressure, cloud cover percentage, air/panels temperature and wind speed. The per unit surface power output is modeled by [12]:

$$96 \quad P_{PV}(t) = \eta \cdot A \cdot I_r(t) \cdot (1 - C_p \cdot (T(t) - 25)) \quad (1)$$

97 where  $\eta$  is the power conversion efficiency of the module (%),  $A$  is the surface area of PV panels ( $m^2$ ),  $I_r$  is the global solar  
 98 radiation ( $kW/m^2$ ) and  $T$  is the outside air temperature ( $^{\circ}C$ ),  $C_p$  is the cell maximum power temperature coefficient (equal to  
 99 0.0035 but it can varies from 0.005 to 0.003 per  $^{\circ}C$  in crystalline silicon).

100 The PV power, solar irradiance and temperature of our lab PV plant have been recorded during three continuous days  
 101 (22/06/2010 - 24/06/2010) and are presented respectively in Fig. 1. The PV power variability is highly correlated with irradiance,  
 102 so as to the temperature, while the PV power uncertainty is almost caused by the irradiance change. Sensed PV power data points  
 103 can be drawn according to sensed irradiance and temperature data points in order to highlight correlations (Fig. 2).

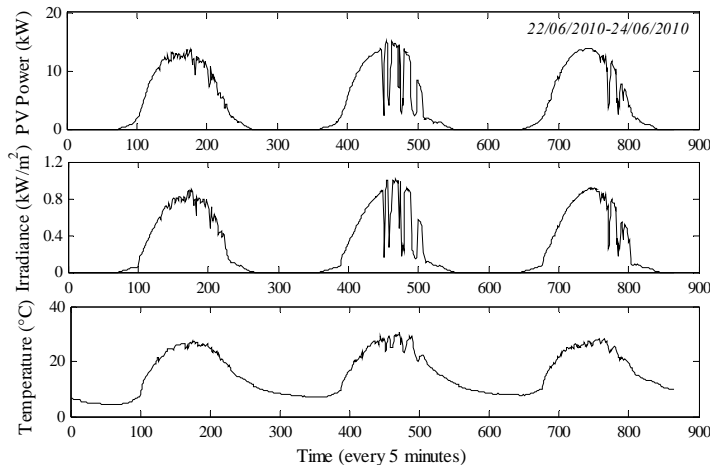


Fig. 1. PV power, solar irradiance and temperature in three continuous days.

104  
 105

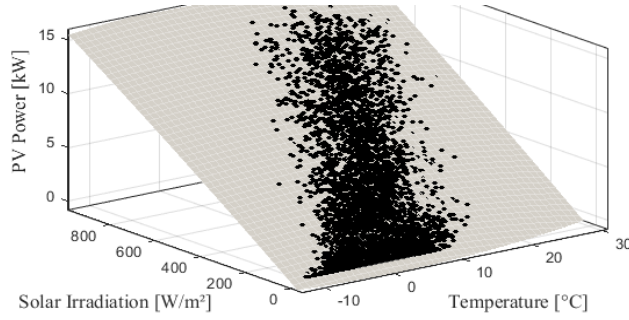


Fig. 2. Irradiance and Temperature vs. Power correlation.

The local load consumption demand is also highly unpredictable and quite random. It depends on different factor, such as the economy, the time, the weather, and other random effects. However, for power system planning and operation, load demand variation and uncertainty analysis are crucial for power flow study or contingency analysis. As for PV production, load demand variations exist in all time scales and system actions are needed for power control in order to maintain the balancing.

### B. Power Forecasting Methodology

#### 1) PV Power Forecasting

In recent decades, several forecasting models of energy production have been published [13-17]. For PV power, one method consists in forecasting solar radiation and then forecasting PV power with a mathematical model of the PV generator. A second one proposes to directly predict the PV power output from environmental data (irradiance, temperature, etc.). Statistical analysis tools are generally used, such as linear/multiple-linear/non-linear regression and autoregressive models that are based on time series regression analysis [18]. These forecasting models rely on modeling relationships between influent inputs and the produced output power. Consequently, mathematical model calibration and parameters adjustment process take a long time. Meanwhile, some intelligent based electrical power generation forecast methods, as expert systems, fuzzy logic, neural networks, are widely used to deal with uncertainties of RES power generation and load demand [13,19].

In daily markets, the hourly PV power output for the next day (day D+1) at time step  $h$  is represented as the sum of a day ahead hourly forecast PV power ( $\tilde{P}_{V_h}$ ) and the forecast error ( $\varepsilon_h^{PV}$ ):

$$P_{V_h} = \tilde{P}_{V_h} + \varepsilon_h^{PV} \quad (2)$$

#### 2) Load Demand Forecasting

For load demand forecast, numerous variables affect directly or indirectly the accuracy. Until now, many methods and models have already been tried out. In [19], several long-term (month or year) load forecasting methods are introduced and are very important for planning and developing future generation, transmission and distribution systems. In [27], a long term probabilistic load forecasting method is proposed with three modernized elements: predictive modeling, scenario analysis, and weather normalization. Long-term and short-term load forecast play important roles in the formulation of secure and reliable operating strategies for the electrical power system. The objective is to improve the forecast accuracy in order to optimize power system planning and to reduce costs.

The day ahead actual load demand at time step  $h$  ( $L_h$ ) is assumed to be the sum of the day ahead forecasted load ( $\tilde{L}_h$ ) and an error ( $\varepsilon_h^L$ ):

$$L_h = \tilde{L}_h + \varepsilon_h^L \quad (3)$$

136 3) Net Demand Forecasting

137 Knowing the PV power forecasting and the load demand forecasting, the net demand forecasting ( $\tilde{ND}_h$ ) for a given time step  
 138  $h$  is expressed as:

$$139 \quad \tilde{ND}_h = \tilde{L}_h - \tilde{P}_{V_h} \quad (4)$$

140 The real net demand ( $ND_h$ ) is composed of the forecasted day ahead ND and a forecast error ( $\varepsilon_h^{ND}$ ):

$$141 \quad ND_h = \tilde{ND}_h + \varepsilon_h^{ND} \quad (5)$$

142 C. Application of Back-Propagation ANN to Forecast

143 In order to predict the net demand errors, as well as PV and load forecast errors, we have developed several back-propagation  
 144 (BP) Artificial Neural Networks (ANN) [22]. Compared with conventional statistical forecasting schemes, ANN has some  
 145 additional advantages, such as simplicity in adaptability to online measurements, data error tolerance and lack of any excess  
 146 information. Since the fundamentals of ANN based predictors can be found in many sources, it will not be recalled again.

147 III. NET DEMAND UNCERTAINTY ANALYSIS

148 A. Net Demand Uncertainty

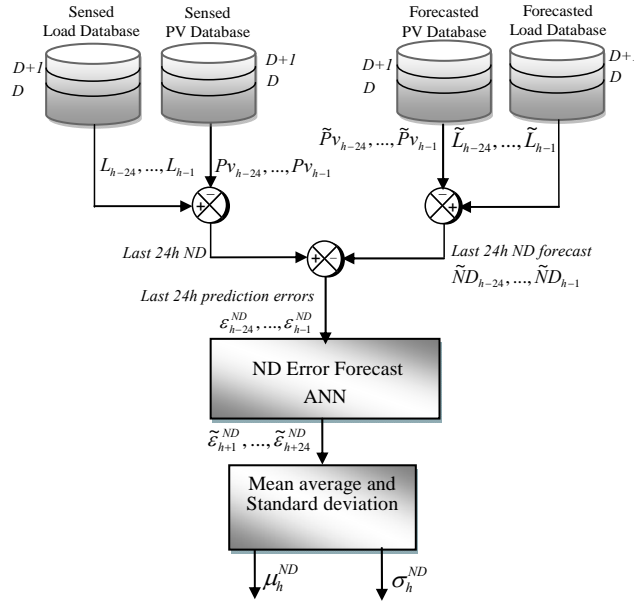


Fig. 3. Net demand uncertainty calculation from ND error forecast.

149 In order to simplify the study, the uncertainties coming from conventional generators and network outages are ignored and  
 150 only load and PV power uncertainties are considered. Then the error of the ND forecasting is representing the ND uncertainty.  
 151 Two possible methods are proposed to calculate the forecasted net demand error.

152 1) First Method: Forecast of the Day-ahead Net Demand Error

153 The real ND is the difference of the sensed load and the sensed PV power. Based on the historical sensed and forecasted  
 154 database of the load demand and PV production, the past forecasted ND is calculated as the difference between past forecasted  
 155 load and past forecasted PV power at time step  $h$ . Then by using past real ND ( $ND_{h-24}, \dots, ND_{h-1}$ ) and also past forecasted ND ( $\tilde{ND}_{h-24}, \dots, \tilde{ND}_{h-1}$ ), the last 24h prediction ND errors are obtained ( $\varepsilon_{h-24}^{ND}, \dots, \varepsilon_{h-1}^{ND}$ ). Hence these data are used to calculate the day-

160 ahead forecast of ND errors  $\tilde{\varepsilon}_h^{ND}$  ( $D+1$ ) (Fig. 3). The obtained ND error forecast can be characterized by the mean and variance  
 161 (respectively,  $\mu_h^{ND}$  and  $\sigma_h^{ND}$ ).

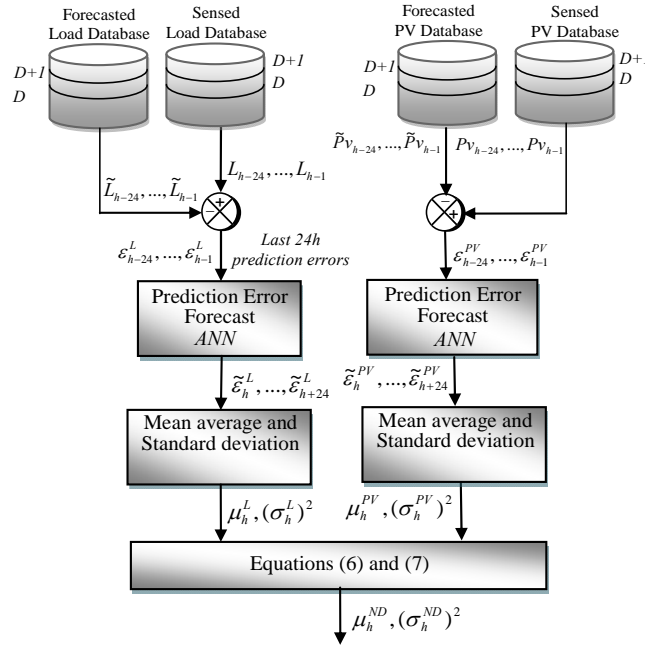
162 *2) Second Method: Calculation from the PV Power and the Load Forecast Errors Estimation*

163 A second method is to define the ND uncertainty as the combination of PV power and load uncertainties. It is generally  
 164 assumed that PV power and load forecast errors are unrelated random variables. So, firstly the day-ahead PV power and load  
 165 forecasting errors ( $\tilde{\varepsilon}_h^{PV}$  and  $\tilde{\varepsilon}_h^L$ ) are estimated independently. Then, last 24-hour load forecast errors and PV power forecast  
 166 errors are calculated as the difference of the sensed load and PV power, and forecasted load and PV power, respectively (Fig. 4).  
 167 The mean values and standard deviations of those forecasting errors can be obtained. Then the ND forecasting error can be  
 168 attained as a new variable which comes from those two independent variables. The new obtained *pdf* is also a normal distribution  
 169 with the following mean and variance [20, 21]:

170 
$$\mu_h^{ND} = \mu_h^L - \mu_h^{PV} \quad (6)$$

171 
$$\sigma_h^{ND} = \sqrt{(\sigma_h^L)^2 + (\sigma_h^{PV})^2} \quad (7)$$

172  $\mu_h^L$  and  $\mu_h^{PV}$  are respectively the mean values of load and PV power forecast errors prediction at time step  $h$ ,  $\sigma_h^L$  and  $\sigma_h^{PV}$  are  
 173 respectively the standard deviation square of the load and PV power forecasted errors prediction.



174  
 175 Fig. 4. Net demand uncertainty calculation from PV power and load forecasting errors prediction.

176 *B. Assessment of the Forecasting Uncertainty*

177 The predicted errors ( $\tilde{\varepsilon}_h^{ND}$ ) of the ND forecast ( $\tilde{ND}_h^{ND}$ ) can be obtained with the normal probability density function (Fig. 5).

178 
$$pdf_h^{ND} = \frac{1}{\sigma_h^{ND} \sqrt{2\pi}} \int_{-\infty}^B e^{-\frac{(\tau - \mu_h^{ND})^2}{2(\sigma_h^{ND})^2}} d\tau = F(B | \mu_h^{ND}, \sigma_h^{ND}) \quad (8)$$

179 The forecasting uncertainty can be represented as upper and lower bound margins around the ND forecast. Bound margins  
 180 ( $B$ ) are extracted by a normal inverse cumulative distribution function for a desired probability index  $x$  (Fig. 5):

$$B = F^{-1}(x | \mu_h^{ND}, \sigma_h^{ND}) = \left\{ B : F(B | \mu_h^{ND}, \sigma_h^{ND}) = x \right\} \quad (9)$$

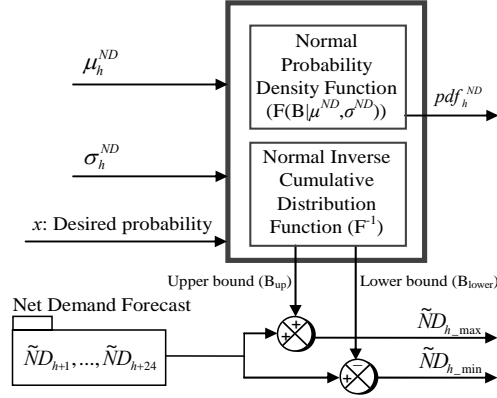


Fig. 5 Net uncertainty calculation at hour  $h$  with a given probability.

#### IV. POWER RESERVE QUANTIFICATION

##### A. Reliability Assessment

Resulting from the uncertainty assessment, the  $pdf$  of the forecasted ND errors in a given time step is considered for the calculation of the power reserve [23]. To estimate the impact of forecast ND uncertainty, two common reliability assessment parameters are used: the loss of load probability (LOLP) and the expected energy not served (EENS) [24-26]. LOLP represents the probability that the load demand ( $L_h$ ) exceeds PV power ( $P_h$ ) at time step  $h$ :

$$LOLP_h = \text{prob}(L_h - P_h > 0) = \int_R^{+\infty} pdf(\tau) d\tau \quad (10)$$

$\text{prob}(L_h - P_h > 0)$  is also the probability that the power reserve ( $R$ ) is insufficient to satisfy the load demand in the time step  $h$ .

Meanwhile, EENS measures the magnitude of the load demand not served:

$$EENS_h = \text{prob}(L_h - P_h > 0) \times (L_h - P_h) \quad (11)$$

where  $(L_h - P_h)$  is the missed power in the time step  $h$ .

In this situation, the grid operator can either disconnect a part of loads or use the power reserve to increase the power production.

After obtaining each of the next 24 hours forecast ND  $pdf_s$ , an hourly day ahead reliability assessment can be attained. Electrical system operators can use this reliability to calculate the system security level.

##### B. Risk-constrained Energy Management

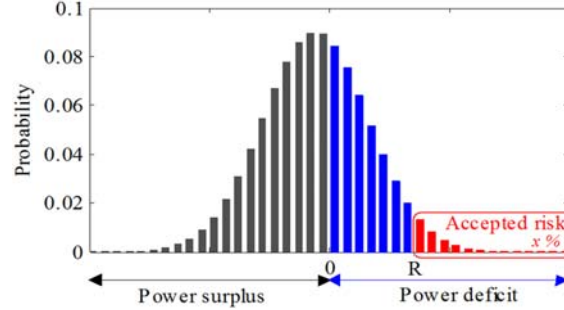
A reserve characteristic according to a risk level and for each time step can be obtained. With a fixed risk index, the operator can then easily quantify the power reserve [9]. As shown in Fig. 6, the sum of the shaded areas represents the accepted risk of violation with  $x$  % of LOLP.  $R$  is the needed power reserve to compensate the remaining power unbalance. So, the reliability assessment can be done with the hourly cumulative distribution function ( $cdf$ ) obtained from the normal difference distribution of ND errors. Then the  $cdf$  represents the probability that the random variable (here the ND error) is less or equal to  $x$ .

This assessment has been made under the assumption of a positive hourly forecasted ND. Otherwise, if the forecasted ND is negative, the reserve power for the same reliability level will be unnecessary (the power generation is more than the load demand). So the reliability has been assessed by considering only positive forecasted ND errors ( $L_h - P_h$ ) for each time step. Then, LOLP is deduced with:



209 
$$LOLP_h = 1 - \text{prob}(L_h - P_h < 0) = 1 - \int_{-\infty}^R \text{pdf}(\tau) d\tau \quad (12)$$

210 When the LOLP equals to the risk index  $x\%$ , the reserve power ( $R$ ) covers the remaining probability that the load demand  
 211 exceeds the PV power generation (blue part in Fig. 6).



212  
 213 Fig. 6. Calculation of power reserve requirements ( $R$ ) based on forecast ND uncertainty ( $\tilde{\varepsilon}_h^{ND}$ ) with  $x\%$  of LOLP, at time step  $h$ .

214 **V. ILLUSTRATIVE CASE STUDY**

215 *A. Presentation and Data Collection*

216 The studied urban microgrid is a 110 kW load peak and is powered with 17 kW PV panels and three micro-gas turbines 30  
 217 kW, 30 kW and 60 kW each. Sensed data from our 17 kW PV plant located on the lab roof have been recorded in 2010 and  
 218 2013. For the load forecasting, past daily French power consumptions have been scaled to obtain per unit values of locally power  
 219 consumption with the same characters and dynamics. A part of this database has been used to design the ANN based forecasting  
 220 tool, a part to assess the estimation quality and a third one to implement the application of the proposed method in a real situation  
 221 [15].

222 The ANN has been trained with past recorded data from the training set to predict hourly PV output power. The efficiency of the  
 223 proposed method is validated by analyzing the normalized Root Mean Square Error ( $nRMSE$ ) and normalized Mean Absolute  
 224 Error ( $nMAE$ ) between predicted values ( $\tilde{y}_k$ ) and measured values ( $y_k$ ):

225 
$$nRMSE = \sqrt{\frac{1}{n} \sum_{i=1}^n (\tilde{y}_k - y_k)^2} \quad (13)$$

226 
$$nMAE = \frac{1}{n} \sum_{i=1}^n |\tilde{y}_k - y_k| \quad (14)$$

227 *B. ANN Based Power Forecast and Net Demand Forecast*

228 *1) ANN based PV Power Forecasting*

- 229 A three-layer ANN has been developed for the PV power generation prediction with:
- 230 - one input layer including last  $n$  hours of measured PV power, of irradiance and of forecasted average temperature (obtained
  - 231 from our local weather information service) (Fig. 7);
  - 232 - one hidden layer with 170 neurons;
  - 233 - one output layer with the 24 predicted PV power points (for each hour).

234 Various hidden layer neurons have been tested until getting an  $nRMSE$  inferior to 5%. First, 60% of previously sensed data  
 235 (representing one year of data) have been used for training the ANN based PV power forecasting tool. Next 20% of sensed data  
 236 are used to create a validation pattern set in order to assess the prediction quality. The test set (with the remaining 20% data) is  
 237 used to implement the forecast error calculation. Obtained  $nRMSE$  and  $nMAE$  for next 24 hours PV power predictions are given

238 in Table I. Predicted errors for 120 test days are given in Fig. 8. Absolute values are less than 0.4 p.u. of the PV power output.  
 239 The largest errors are in the middle of the day when the PV power production is the highest.

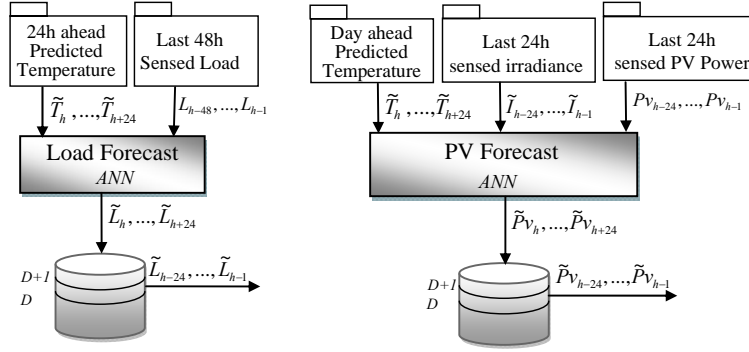


Fig. 7. PV power, load forecasting and errors prediction with ANN.

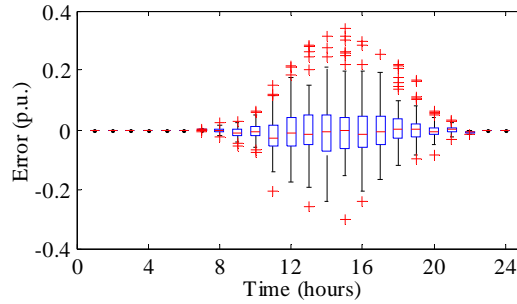


Fig. 8. PV power prediction errors on 120 test days.

TABLE I. Errors of the PV Power Forecast with ANN

	$nRMSE$ [%]	$nMAE$ [%]
Training Set	4.67	2.69
Validation Set	5.58	3.13
Test Set	5.95	3.12

245  
 246 *2) ANN based Load Forecasting*

247 Another neural network has been used for load forecast. The load demand prediction model includes: an input layer with last  
 248 48 hours load demand measurements and predicted temperatures for next 24 hours, one hidden layer with 70 neurons (in order to  
 249 get an  $nRMSE$  inferior to 4%) and an output layer that predicts next 24 hours load demand. 60% of available data are used for the  
 250 neural network training, 20% for the validation and 20% for tests. The predicted errors for 120 test days are shown in Fig. 9. As it  
 251 can be seen, the largest forecast error occurs at 8:00 and 18:00. Yet the total absolute errors are less than 0.2 p.u. of the load  
 252 demand. Obtained results of  $nRMSE$  and  $nMAE$  are listed in Table II.

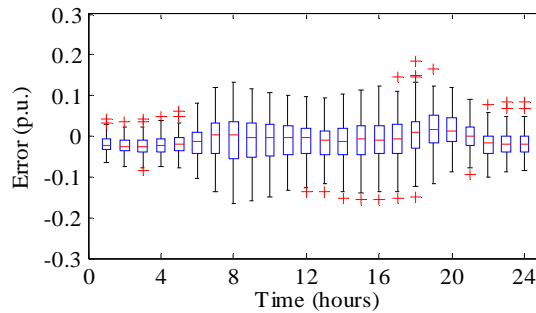


Fig. 9. Load prediction on 120 test days.

TABLE II. ERRORS OF THE LOAD DEMAND FORECAST WITH ANN

	<i>nRMSE [%]</i>	<i>nMAE [%]</i>
Training Set	3.18	2.45
Validation Set	3.57	2.76
Test Set	3.67	2.84

256

### 257 3) Net Demand Uncertainty

#### 258 a) First Method: Direct Net Demand Forecast

259 Following the method highlighted in Fig. 3, another ANN is applied for ND errors forecast: an input layer with last 24 hours  
 260 predicted net demand errors, one hidden layer with 70 neurons and an output layer that predicts next 24 hours forecasted net  
 261 errors.

262 Application of the first method (Fig. 3) for the time step at 12 am gives:  $\mu_{12}^{ND} = -0.1282$ ,  $\sigma_{12}^{ND} = 1.781$  and the frequency  
 263 distribution is shown on Fig 10(a).

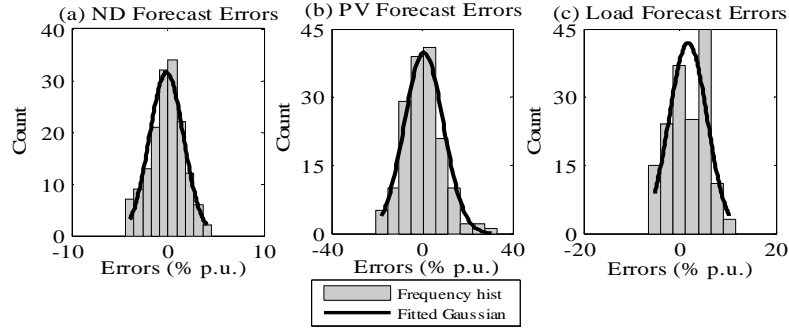
#### 264 b) Second Method: Calculation of the PV Power and the Load Forecast Errors

265 Two additional three-layer ANN are used to forecast the errors of PV power and load forecasts. Outputs are the predicted  
 266 forecasting errors corresponding to the hourly predicted PV power and load, while inputs are the last 24 forecasting errors of PV  
 267 power and loads.

268 For each hour, the mean and standard deviation have been calculated and the corresponding normal *pdf* has been computed.  
 269 As example, the distributions and normal *pdf* of predicted errors of PV power and load errors forecast at 12 am are shown

270 respectively in Fig. 10(b) with obtained parameters:  $\mu_{12}^{PV} = -0.0353$ ,  $\sigma_{12}^{PV} = 0.01571$  for the PV forecast error ( $\epsilon_{h-12}^{PV}$ ) and in

271 Fig. 10(c) with obtained parameters:  $\mu_{12}^L = -0.0353$ ,  $\sigma_{12}^L = 0.01571$  for the load forecast error ( $\epsilon_{h-12}^L$ ).



272 Fig. 10. Frequency distribution histograms and fitted Gaussian functions at 12 am.  
 273

#### 274 C. Forecasting Uncertainty Assessment

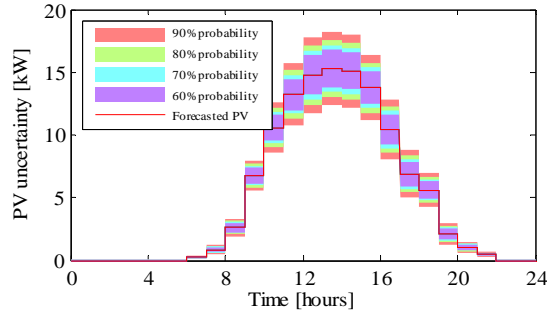
275 By applying both proposed methods, the uncertainties of PV power forecasting, load forecasting and net forecasting with  
 276 various probability indices (from 90% to 60%) in a random day are represented as a function of the forecasting data and the  
 277 predicted errors of forecasting. In order to simplify the explanation, results are given with the second method (corresponding to  
 278 Fig. 5).

279 As shown in Fig. 11, the uncertainty of PV power forecasting is higher in the middle of the day, when the PV system generates  
 280 the highest power. While in the morning (from 6:00 to 10:00) and afternoon (from 17:00 to 21:00), the uncertainty is smaller.  
 281 Obviously, PV power forecasting uncertainty increases, and decreases with PV power increase and decrease respectively. Also,  
 282 the uncertainty is increased when the time horizon is larger. For example, at 10:00 and at 17:00 power outputs are almost at the

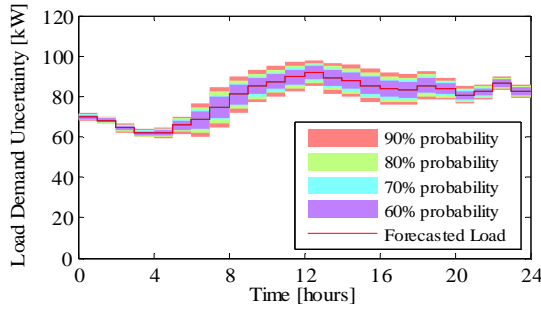
283 same level (about 6.5 kW), but uncertainty is larger at 17:00 than at 9:00. The load forecasting has the same variation trend (Fig.  
 284 12).

285 Fig. 13 depicts the obtained ND uncertainty with the first method. If the forecasted ND is positive, then additional power  
 286 sources have to be programmed to cover the difference. Otherwise, if forecasted ND is negative then three actions must be  
 287 considered to meet the low forecasted demand:

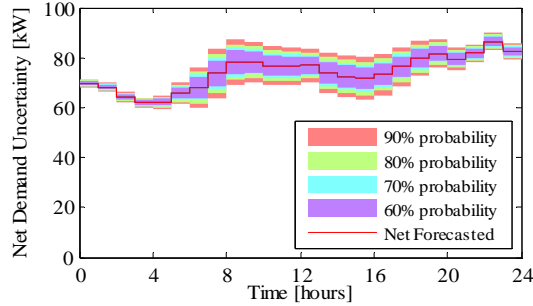
- 288 - A part of PV power generators must be switched off (or can work at a sub-optimal level).
- 289 - Controllable loads (as electrical vehicles, heating loads.) must be switched on to absorb excess available power.
- 290 - Export the available excess energy to the main grid.



291 Fig. 11. PV forecasting with uncertainty (a random day).  
 292



293 Fig. 12. Load forecasting with uncertainty (a random day).  
 294

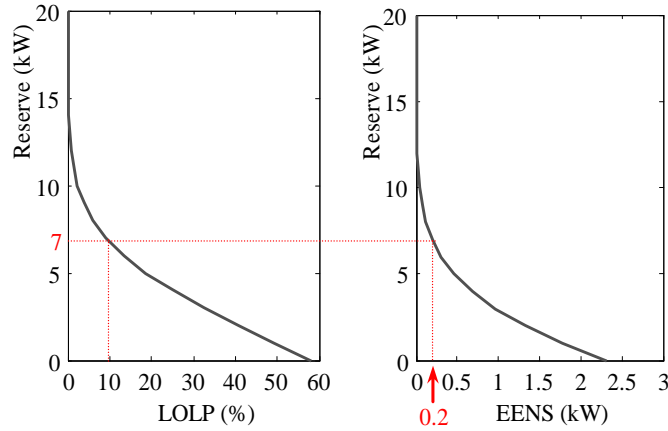


295 Fig. 13. Next 24 hours NFD with uncertainty (a random day).  
 296

297 *D. Power Reserve Calculation with Fixed Risk Indices*

298 The forecasted ND uncertainty assessment has been done with the hourly cumulative distribution function (*cdf*) obtained from  
 299 the ND forecast errors. Then, the hourly risk/reserve curve takes into account all the errors from the *cdf*s. Since the forecast ND  
 300 errors can be expressed as an  $x$  % of the rated power, the PR can be drawn according to the LOLP. Fig. shows the required PR  
 301 variation according to LOLP and EENS (with the second method in Section III). Therefore, an operating PR under  $x$  % of LOLP  
 302 would cover a part of the forecast ND uncertainty. For example, with 10% of LOLP, the reserve power will be 7 kW and the

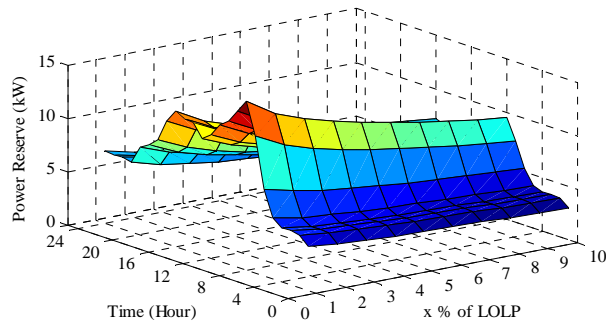
303 EENS will be 0.2 kW. In general, this operating reserve is limited not only by the risk indices but also by the availability of micro-  
 304 gas turbines.



305  
 306 Fig. 14. Risk/reserve curve for  $LOLP_{h+12}$  and  $EENS_{h+12}$  at 12:00.

307 On Fig. 15, an assessment of hourly reserve power required with the second method for different LOLP has been deduced.  
 308 Much more reserve will be needed when the LOLP rate is very low, which means a high security level. While less reserve power  
 309 will be needed with a high LOLP rate, but then the risk will be higher. For example with 1% of LOLP, the necessary PR will be  
 310 14 kW (EENS is almost zero) at 12:00 am, while the necessary reserve power will be 7 kW with a 10% of LOLP and EENS  
 311 increases to 0.25 kWh.

312 If a constant LOLP rate is set, the power reserve for each hour can be obtained. As shown in Fig. 16, with a 1% of LOLP, more  
 313 power reserve is needed in the middle of the day when larger PV power is generated. Moreover, power reserve with the second  
 314 method is higher than the method with direct ND forecast. The most likely explanation of this result is because the load forecast  
 315 uncertainty and PV forecast uncertainty are not totally independent. Sharing a common temperature, integrated PV power  
 316 uncertainty and load uncertainty is greater than the direct ND forecast uncertainty. This result can be used for power dispatch  
 317 management.



318  
 319 Fig. 15. Required power reserve for each hour with  $x\%$  LOLP.

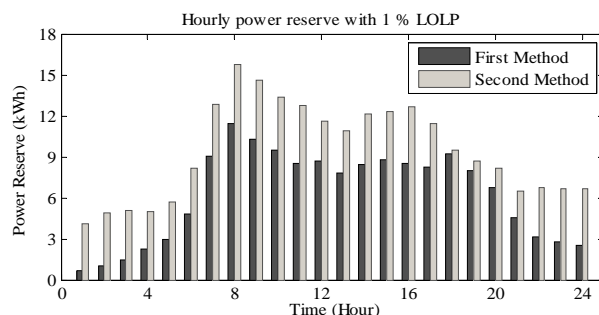


Fig. 16. Hourly power reserve with two different methods (1% of LOLP).

## VI.CONCLUSION

This work proposed a new technique to quantify the power reserve of a microgrid by taking into account the PV power forecasting uncertainty and load forecasting uncertainty. In order to assess these uncertainties, a three-layer BP ANN is used to estimate errors of PV power and load forecastings. Two methods are proposed to obtain the ND forecast uncertainties. With the first method, a probabilistic model is proposed to forecast ND uncertainty distribution by integrating the uncertainties from both PV power and load. The other method is desired to directly forecast the ND errors. The power reserve quantification results demonstrate that with a fixed risk index, the power reserve for next day or next 24 hours can be evaluated to cover the risk.

As the uncertainty from forecasting errors increases with time horizon, future research works are oriented toward the implementation of the intraday adjustment. The dispatch of the calculated power reserve onto micro-gas turbines, controllable loads and also new "PV based active power generators" is also an interesting way to pave.

## ACKNOWLEDGMENT

The authors would like to thank the China Scholarship Council and Centrale Lille for their cofounding supports

## REFERENCES

- [1] E. Romero-Cadaval, B. Francois, M. Malinowski, and Q.-C. Zhong, "Grid-Connected Photovoltaic Plants: An Alternative Energy Source, Replacing Conventional Sources," *Industrial Electronics Magazine, IEEE*, vol. 9, pp. 18-32, 2015.
- [2] A. Ipakchi and F. Albuyeh, "Grid of the future," *Power and Energy Magazine, IEEE*, vol. 7, pp. 52-62, 2009.
- [3] F. D. Galiana, F. Bouffard, J. M. Arroyo, and J. F. Restrepo, "Scheduling and pricing of coupled energy and primary, secondary, and tertiary reserves," *Proceedings of the IEEE*, vol. 93, pp. 1970-1983, 2005.
- [4] A. Mills, "Integrating Solar PV in Utility System Operations," *Argonne National Laboratory, LBNL-6525E, Mar*, 2014.
- [5] A. Sobu and G. Wu, "Dynamic optimal schedule management method for microgrid system considering forecast errors of renewable power generations," in *Power System Technology (POWERCON), 2012 IEEE International Conference on*, 2012, pp. 1-6.
- [6] M.-M. Buzau and B. Francois, "Quantification of operating power reserve through uncertainty analysis of a microgrid operating with wind generation," in *Electrical Sciences and Technologies in Maghreb (CISTEM), 2014 International Conference on*, 2014, pp. 1-8.
- [7] X. Yan, B. Francois, and D. Abbes, "Operating power reserve quantification through PV generation uncertainty analysis of a microgrid," in *PowerTech, 2015 IEEE Eindhoven*, 2015, pp. 1-6.
- [8] G. Delille, B. François, and G. Malarange, "Dynamic frequency control support by energy storage to reduce the impact of wind and solar generation on isolated power system's inertia," *IEEE Transactions on Sustainable Energy* vol. 3, pp. 931-939, 2012.
- [9] K. De Vosa, A. G. Petoussis, J. Driesen, R. Belman, "Revision of reserve requirements following wind power integration in island power systems", *Renewable Energy*, vol. 50, Feb. 2013, pp. 268-279
- [10] G. Sansavini, R. Piccinelli, L.R. Golea, E. Zio, "A stochastic framework for uncertainty analysis in electric power transmission systems with wind generation", *Renewable Energy*, vol. 64, April 2014, pp. 71-81.
- [11] H. Yang, J. Qiu, K. Meng, J. Hua Zhao, Z. Yang Dong, M. Lai, "Insurance strategy for mitigating power system operational risk introduced by wind power forecasting uncertainty", *Renewable Energy*, vol. 89, April 2016, Pages 606-615

- 355 [12] M. Fuentes, G. Nofuentes, J. Aguilera, D. Talavera, and M. Castro, "Application and validation of algebraic methods to predict the behaviour of crystalline  
356 silicon PV modules in Mediterranean climates," *Solar Energy*, vol. 81, pp. 1396-1408, 2007.
- 357 [13] B. Espinar, J.-L. Aznarte, R. Girard, A. M. Moussa, and G. Kariniotakis, "Photovoltaic Forecasting: A state of the art," in *Proceedings 5th European PV-  
358 Hybrid and Mini-Grid Conference*, 2010.
- 359 [14] X. Yan, B. Francois, and D. Abbes, "Solar radiation forecasting using artificial neural network for local power reserve," in *Electrical Sciences and  
360 Technologies in Maghreb (CISTEM), 2014 International Conference on*, 2014, pp. 1-6.
- 361 [15] A. G. C. de Rocha Vaz, "Photovoltaic forecasting with artificial neural networks," *University of Lisbon, 2014 (MSc thesis)* Retrieved from,  
362 [http://repositorio.ul.pt/bitstream/10451/11405/1/ulfc107351\\_tm\\_Andre\\_Vaz.pdf](http://repositorio.ul.pt/bitstream/10451/11405/1/ulfc107351_tm_Andre_Vaz.pdf), 2014.
- 363 [16] A. A. Mohammed, W. Yaqub, and Z. Aung, "Probabilistic Forecasting of Solar Power: An Ensemble Learning Approach," in *Intelligent Decision  
364 Technologies*, ed: Springer, 2015, pp. 449-458.
- 365 [17] F. Golestaneh, H. B. Gooi, and P. Pinson, "Generation and evaluation of space-time trajectories of photovoltaic power," *Applied Energy*, vol. 176, pp. 80-  
366 91, 2016.
- 367 [18] M. G. De Giorgi, P. M. Congedo, and M. Malvoni, "Photovoltaic power forecasting using statistical methods: impact of weather data," *IET Science,  
368 Measurement & Technology*, vol. 8, pp. 90-97, 2014.
- 369 [19] L. Ghods and M. Kalantar, "Different methods of long-term electric load demand forecasting; a comprehensive review," *Iranian Journal of Electrical &  
370 Electronic Engineering*, vol. 7, p. 249, 2011.
- 371 [20] M. A. Ortega-Vazquez and D. S. Kirschen, "Estimating the spinning reserve requirements in systems with significant wind power generation penetration,"  
372 *Power Systems, IEEE Transactions on*, vol. 24, pp. 114-124, 2009.
- 373 [21] F. Bouffard and F. D. Galiana, "Stochastic security for operations planning with significant wind power generation," in *Power and Energy Society General  
374 Meeting-Conversion and Delivery of Electrical Energy in the 21st Century, 2008 IEEE*, 2008, pp. 1-11.
- 375 [22] B. Francois, "Orthogonal considerations in the design of neural networks for function approximation," *Mathematics and computers in simulation*, vol. 41,  
376 pp. 95-108, 1996.
- 377 [23] H. Holttinen, M. Milligan, E. Ela, N. Menemenlis, J. Dobschinski, B. Rawn, *et al.*, "Methodologies to determine operating reserves due to increased wind  
378 power," in *Power and Energy Society General Meeting (PES), 2013 IEEE*, 2013, pp. 1-10.
- 379 [24] Y.-F. Li and E. Zio, "A multi-state model for the reliability assessment of a distributed generation system via universal generating function," *Reliability  
380 Engineering & System Safety*, vol. 106, pp. 28-36, 2012.
- 381 [25] M. Wang and H. Gooi, "Spinning reserve estimation in microgrids," *Power Systems, IEEE Transactions on*, vol. 26, pp. 1164-1174, 2011.
- 382 [26] G. Liu and K. Tomsovic, "Quantifying spinning reserve in systems with significant wind power penetration," *Power Systems, IEEE Transactions on*, vol.  
383 27, pp. 2385-2393, 2012.
- 384 [27] T. Hong, J. Wilson, and J. Xie, "Long term probabilistic load forecasting and normalization with hourly information," *IEEE Transactions on Smart Grid*,  
385 vol. 5, pp. 456-462, 2014.

386

387